Rapid Communications

Evidence for the decay $B^0 \to p\bar{p}\pi^0$

B. Pal,[3] I. Adachi,[16,12] K. Adamczyk,[59] H. Aihara,[82] D. M. Asner,[3] H. Atmacan,[72] V. Aulchenko,[4,62] T. Aushev,[51] R. Ayad,[76] V. Babu,[77] I. Badhrees,[76,34] V. Bansal,[63] P. Behera,[23] C. Beleño,[11] M. Berger,[73] V. Bhardwaj,[20] B. Bhuyan,[21] T. Bilka,[5] J. Biswal,[31] A. Bobrov,[4,62] A. Bozek,[59] M. Bračko,[45,31] T. E. Browder,[15] M. Campajola,[28,54] L. Cao,[32] D. Červenkov,[5] V. Chekelian,[46] A. Chen,[56] B. G. Cheon,[14] K. Chilikin,[40] K. Cho,[35] S.-K. Choi,[13] Y. Choi,[74] D. Cinabro,[86] S. Cunliffe,[8] S. Di Carlo,[38] Z. Doležal,[5] T. V. Dong,[16,12] D. Dossett,[47] S. Eidelman,[4,62,40] D. Epifanov,[4,62] J. E. Fast,[63] T. Ferber,[8] B. G. Fulsom,[63] R. Garg,[64] V. Gaur,[85] N. Gabyshev,[4,62] A. Garmash,[4,62] A. Giri,[22] P. Goldenzweig,[32] Y. Guan,[24,16] J. Haba,[16,12] T. Hara,[16,12] K. Hayasaka,[61] H. Hayashii,[55] W.-S. Hou,[58] C.-L. Hsu,[75] T. Iijima,[53,52] K. Inami,[52] A. Ishikawa,[80] R. Itoh,[16,12] M. Iwasaki,[89] Y. Iwasaki,[16] W. W. Jacobs,[24] S. Jia,[2] Y. Jin,[82] D. Joffe,[33] K. K. Joo,[6] A. B. Kaliyar,[23] G. Karyan,[8] H. Kichimi,[16] C. Kiesling,[46] C. H. Kim,[14] D. Y. Kim,[71] K. T. Kim,[36] S. H. Kim,[14] K. Kinoshita,[7] P. Kodyš,[5] S. Korpar,[45,31] D. Kotchetkov,[15] P. Križan,[41,31] R. Kroeger,[48] P. Krokovny,[4,62] R. Kulasiri,[33] Y.-J. Kwon,[88] J. Y. Lee,[69] S. C. Lee,[37] L. K. Li,[25] Y. B. Li,[65] L. Li Gioi,[46] J. Libby,[23] D. Liventsev,[85,16] P.-C. Lu,[58] T. Luo,[10] J. MacNaughton,[49] C. MacQueen,[47] M. Masuda,[81] T. Matsuda,[49] D. Matvienko,[4,62,40] M. Merola,[28,54] K. Miyabayashi,[55] H. Miyata,[61] R. Mizuk,[40,50,51] G. B. Mohanty,[77] M. Nakao,[16,12] K. J. Nath,[21] M. Nayak,[86,16] N. K. Nisar,[66] S. Nishida,[16,12] K. Nishimura,[15] S. Ogawa,[79] H. Ono,[60,61] Y. Onuki,[82] P. Pakhlov,[40,50] G. Pakhlova,[40,51] S. Pardi,[28] S.-H. Park,[88] S. Patra,[20] S. Paul,[78] T. K. Pedlar,[43] R. Pestotnik,[31] L. E. Piilonen,[85] V. Popov,[40,51] E. Prencipe,[18] A. Rostomyan,[8] G. Russo,[28] Y. Sakai,[16,12] M. Salehi,[44,42] S. Sandilya,[7] T. Sanuki,[80] V. Savinov,[66] O. Schneider,[39] G. Schnell,[1,19] J. Schueler,[15] C. Schwanda,[26] A. J. Schwartz,[7] Y. Seino,[61] K. Senyo,[87] M. E. Sevior,[47] C. P. Shen,[2] J.-G. Shiu,[58] F. Simon,[46] A. Sokolov,[27] E. Solovieva,[40] M. Starič,[31] Z. S. Stottler,[85] J. F. Strube,[63] T. Sumiyoshi,[84] W. Sutcliffe,[32] M. Takizawa,[70,17,67] U. Tamponi,[29] K. Tanida,[30] F. Tenchini,[8] M. Uchida,[83] T. Uglov,[40,51] S. Uno,[16,12] P. Urquijo,[47] R. Van Tonder,[32] G. Varner,[15] A. Vinokurova,[4,62] B. Wang,[46] C. H. Wang,[57] M.-Z. Wang,[58] P. Wang,[25] M. Watanabe,[61] S. Watanuki,[80] E. Won,[36] S. B. Yang,[36] H. Ye,[8] J. Yelton,[9] Y. Yusa,[61] J. Zhang,[25] Z. P. Zhang,[68] V. Zhilich,[4,62] and V. Zhukova[40]

(Belle Collaboration)

[1]*University of the Basque Country UPV/EHU, 48080 Bilbao, Spain*
[2]*Beihang University, Beijing 100191, China*
[3]*Brookhaven National Laboratory, Upton, New York 11973, USA*
[4]*Budker Institute of Nuclear Physics SB RAS, Novosibirsk 630090, Russia*
[5]*Faculty of Mathematics and Physics, Charles University, 121 16 Prague, Czech Republic*
[6]*Chonnam National University, Kwangju 660-701, South Korea*
[7]*University of Cincinnati, Cincinnati, Ohio 45221, USA*
[8]*Deutsches Elektronen–Synchrotron, 22607 Hamburg, Germany*
[9]*University of Florida, Gainesville, Florida 32611, USA*
[10]*Key Laboratory of Nuclear Physics and Ion-beam Application (MOE) and Institute of Modern Physics, Fudan University, Shanghai 200443, China*
[11]*II. Physikalisches Institut, Georg-August-Universität Göttingen, 37073 Göttingen, Germany*
[12]*SOKENDAI (The Graduate University for Advanced Studies), Hayama 240-0193, Japan*
[13]*Gyeongsang National University, Chinju 660-701, South Korea*
[14]*Hanyang University, Seoul 133-791, South Korea*
[15]*University of Hawaii, Honolulu, Hawaii 96822, USA*
[16]*High Energy Accelerator Research Organization (KEK), Tsukuba 305-0801, Japan*
[17]*J-PARC Branch, KEK Theory Center, High Energy Accelerator Research Organization (KEK), Tsukuba 305-0801, Japan*
[18]*Forschungszentrum Jülich, 52425 Jülich, Germany*
[19]*IKERBASQUE, Basque Foundation for Science, 48013 Bilbao, Spain*
[20]*Indian Institute of Science Education and Research Mohali, SAS Nagar, 140306, India*
[21]*Indian Institute of Technology Guwahati, Assam 781039, India*
[22]*Indian Institute of Technology Hyderabad, Telangana 502285, India*
[23]*Indian Institute of Technology Madras, Chennai 600036, India*
[24]*Indiana University, Bloomington, Indiana 47408, USA*
[25]*Institute of High Energy Physics, Chinese Academy of Sciences, Beijing 100049, China*
[26]*Institute of High Energy Physics, Vienna 1050, Austria*
[27]*Institute for High Energy Physics, Protvino 142281, Russia*
[28]*INFN—Sezione di Napoli, 80126 Napoli, Italy*

[29]*INFN—Sezione di Torino, 10125 Torino, Italy*
[30]*Advanced Science Research Center, Japan Atomic Energy Agency, Naka 319-1195, Japan*
[31]*J. Stefan Institute, 1000 Ljubljana, Slovenia*
[32]*Institut für Experimentelle Teilchenphysik, Karlsruher Institut für Technologie, 76131 Karlsruhe, Germany*
[33]*Kennesaw State University, Kennesaw, Georgia 30144, USA*
[34]*King Abdulaziz City for Science and Technology, Riyadh 11442, Saudi Arabia*
[35]*Korea Institute of Science and Technology Information, Daejeon 305-806, South Korea*
[36]*Korea University, Seoul 136-713, South Korea*
[37]*Kyungpook National University, Daegu 702-701, South Korea*
[38]*LAL, Univ. Paris-Sud, CNRS/IN2P3, Université Paris-Saclay, Orsay, France*
[39]*École Polytechnique Fédérale de Lausanne (EPFL), Lausanne 1015, France*
[40]*P.N. Lebedev Physical Institute of the Russian Academy of Sciences, Moscow 119991, Russia*
[41]*Faculty of Mathematics and Physics, University of Ljubljana, 1000 Ljubljana, Slovenia*
[42]*Ludwig Maximilians University, 80539 Munich, Russia*
[43]*Luther College, Decorah, Iowa 52101, USA*
[44]*University of Malaya, 50603 Kuala Lumpur, Malaysia*
[45]*University of Maribor, 2000 Maribor, Slovenia*
[46]*Max-Planck-Institut für Physik, 80805 München, Germany*
[47]*School of Physics, University of Melbourne, Victoria 3010, Australia*
[48]*University of Mississippi, University, Mississippi 38677, USA*
[49]*University of Miyazaki, Miyazaki 889-2192, Japan*
[50]*Moscow Physical Engineering Institute, Moscow 115409, Russia*
[51]*Moscow Institute of Physics and Technology, Moscow Region 141700, Russia*
[52]*Graduate School of Science, Nagoya University, Nagoya 464-8602, Japan*
[53]*Kobayashi-Maskawa Institute, Nagoya University, Nagoya 464-8602, Japan*
[54]*Università di Napoli Federico II, 80055 Napoli, Italy*
[55]*Nara Women's University, Nara 630-8506, Japan*
[56]*National Central University, Chung-li 32054, Taiwan*
[57]*National United University, Miao Li 36003, China*
[58]*Department of Physics, National Taiwan University, Taipei 10617, Taiwan*
[59]*H. Niewodniczanski Institute of Nuclear Physics, Krakow 31-342, Poland*
[60]*Nippon Dental University, Niigata 951-8580, Japan*
[61]*Niigata University, Niigata 950-2181, Japan*
[62]*Novosibirsk State University, Novosibirsk 630090, Russia*
[63]*Pacific Northwest National Laboratory, Richland, Washington 99352, USA*
[64]*Panjab University, Chandigarh 160014, India*
[65]*Peking University, Beijing 100871, China*
[66]*University of Pittsburgh, Pittsburgh, Pennsylvania 15260, USA*
[67]*Theoretical Research Division, Nishina Center, RIKEN, Saitama 351-0198, Japan*
[68]*University of Science and Technology of China, Hefei 230026, China*
[69]*Seoul National University, Seoul 151-742, South Korea*
[70]*Showa Pharmaceutical University, Tokyo 194-8543, Japan*
[71]*Soongsil University, Seoul 156-743, South Korea*
[72]*University of South Carolina, Columbia, South Carolina 29208, USA*
[73]*Stefan Meyer Institute for Subatomic Physics, Vienna 1090, Austria*
[74]*Sungkyunkwan University, Suwon 440-746, South Korea*
[75]*School of Physics, University of Sydney, New South Wales 2006, Australia*
[76]*Department of Physics, Faculty of Science, University of Tabuk, Tabuk 71451, Saudi Arabia*
[77]*Tata Institute of Fundamental Research, Mumbai 400005, India*
[78]*Department of Physics, Technische Universität München, 85748 Garching, Germany*
[79]*Toho University, Funabashi 274-8510, Japan*
[80]*Department of Physics, Tohoku University, Sendai 980-8578, Japan*
[81]*Earthquake Research Institute, University of Tokyo, Tokyo 113-0032, Japan*
[82]*Department of Physics, University of Tokyo, Tokyo 113-0033, Japan*
[83]*Tokyo Institute of Technology, Tokyo 152-8550, Japan*
[84]*Tokyo Metropolitan University, Tokyo 192-0397, Japan*
[85]*Virginia Polytechnic Institute and State University, Blacksburg, Virginia 24061, USA*
[86]*Wayne State University, Detroit, Michigan 48202, USA*
[87]*Yamagata University, Yamagata 990-8560, Japan*

[88]Yonsei University, Seoul 120-749, South Korea
[89]Osaka City University, Osaka 558-8585, Japan

(Received 11 April 2019; published 28 May 2019)

We report a search for the charmless baryonic decay $B^0 \to p\bar{p}\pi^0$ with a data sample corresponding to an integrated luminosity of 711 fb^{-1} containing $(772 \pm 10) \times 10^6$ $B\bar{B}$ pairs. The data were collected by the Belle experiment running on the $\Upsilon(4S)$ resonance at the KEKB e^+e^- collider. We measure a branching fraction $\mathcal{B}(B^0 \to p\bar{p}\pi^0) = (5.0 \pm 1.8 \pm 0.6) \times 10^{-7}$, where the first uncertainty is statistical and the second is systematic. The signal has a significance of 3.1 standard deviations and constitutes the first evidence for this decay mode. We also search for the intermediate two-body decays $B^0 \to \Delta^+\bar{p}$ and $B^0 \to \bar{\Delta}^- p$, and set an upper limit on the branching fraction, $\mathcal{B}(B^0 \to \Delta^+\bar{p}) + \mathcal{B}(B^0 \to \bar{\Delta}^- p) < 1.6 \times 10^{-6}$ at 90% confidence level.

DOI: 10.1103/PhysRevD.99.091104

The first observed charmless baryonic B decay was $B^+ \to p\bar{p}K^+$ [1]. Following this first observation, many other charmless baryonic B decays have been found [2]. Except for $B^+ \to p\Lambda\pi^0$ and $p\Lambda\gamma$ decays, all the channels reported to date are entirely reconstructed from charged particles in the final state. A noticeable hierarchy is also observed in the branching fractions of these decays: three-body decays are usually more frequent than their two-body counterparts but less frequent than four-body decays [3,4]. This phenomenon can be understood in terms of the so-called "threshold effect," which refers to the fact that the B meson prefers to decay into a dibaryon pair with low invariant mass accompanied by a fast recoil meson [3,5,6]. This peaking behavior was unexpected, and has led to various speculations about possible mechanisms [7–9]. Studying additional three-body baryonic decays might provide a better understanding of the dynamics of B decays and the aforementioned threshold effect. These decays are also useful for CP violation studies [10].

This paper reports a search for a three-body charmless baryonic B^0 decays to the $p\bar{p}\pi^0$ final state [11] using a data set corresponding to an integrated luminosity of 711 fb^{-1} collected with the Belle detector [12] at the $\Upsilon(4S)$ resonance at the KEKB asymmetric-energy e^+e^- (3.5 on 8.0 GeV) collider [13]. So far, the decay $B^0 \to p\bar{p}\pi^0$ has not been studied by any experiment. No theoretical prediction for the branching fraction of this process is yet available. A glance at the known branching fractions for B decays [2] shows the three-body charmless baryonic decays to occur in the several times 10^{-6} range, indicating that the discovery of the mode $B^0 \to p\bar{p}\pi^0$ might be possible with the currently available data set.

The Belle detector is a large-solid-angle magnetic spectrometer consisting of a silicon vertex detector (SVD), a 50-layer central drift chamber (CDC), an array of aerogel threshold Cherenkov counters (ACC), a barrel-like arrangement of time-of-flight scintillation counters (TOF), and an electromagnetic calorimeter (ECL) comprising CsI(Tl) crystals. These detector components are located inside a superconducting solenoid coil that provides a 1.5 T magnetic field. An iron flux-return located outside the coil is instrumented to detect K_L^0 mesons and to identify muons. Two inner detector configurations were used: a 2.0 cm radius beampipe and a three-layer SVD were used for the first 152×10^6 $B\bar{B}$ pairs of data, while a 1.5 cm radius beampipe, a four-layer SVD, and a small-cell inner drift chamber were used for the remaining 620×10^6 $B\bar{B}$ pairs of data. The detector is described in detail in Ref. [12]. Event selection requirements are optimized using Monte Carlo (MC) simulations. MC events are generated using EvtGen [14], and the detector response is modeled using Geant3 [15]. Final-state radiation is taken into account using the Photos package [16].

The reconstruction of $B^0 \to p\bar{p}\pi^0$ proceeds by first reconstructing $\pi^0 \to \gamma\gamma$ candidates. An ECL cluster not matched to any track in the CDC is identified as a photon candidate. Such candidates are required to have an energy greater than 50 MeV in the barrel region and greater than 100 MeV in the end-cap regions, where the barrel region covers the polar angle $32° < \theta < 130°$ and the end-cap regions cover the ranges $12° < \theta < 32°$ and $130° < \theta < 157°$. To reject showers produced by neutral hadrons, the energy deposited in the 3×3 array of ECL crystals centered on the crystal with the highest energy must exceed 80% of the energy deposited in the corresponding 5×5 array of crystals. We require that the $\gamma\gamma$ invariant mass be within 20 MeV/c^2 (about 3.5σ in resolution) of the π^0 mass [2]. To improve the π^0 momentum resolution, we perform a mass-constrained fit and require that the resulting χ^2 be less than 30. This requirement is relatively loose, retaining more than 99% of candidates.

We subsequently combine π^0 candidates with two oppositely charged tracks, identified as a proton-antiproton

pair. Such tracks are identified using requirements on the distance of closest approach with respect to the interaction point along the z axis (antiparallel to the e^+ beam) of $|dz| < 3.0$ cm, and in the transverse plane of $dr < 0.3$ cm. In addition, charged tracks are required to have a minimum number of SVD hits (>2 along the z axis and >1 in the transverse direction). Particle identification is achieved using information from the CDC, the TOF, and the ACC subdetectors. This information is combined to form a hadron likelihood $\mathcal{L}_h$; a charged track with likelihood ratios of $\mathcal{L}_p/(\mathcal{L}_p + \mathcal{L}_K) > 0.9$ and $\mathcal{L}_p/(\mathcal{L}_p + \mathcal{L}_\pi) > 0.9$ is regarded as a proton or antiproton. Furthermore, we reject tracks consistent with either the electron or muon hypothesis. The proton identification efficiency is 75% and the probability for a kaon (pion) to be misidentified as a proton is 6% (2%).

Candidate B^0 mesons are identified using the beam-energy-constrained mass, $M_{\rm bc} = \sqrt{E^2_{\rm beam} - |\vec{p}_B c|^2}/c^2$, and the energy difference $\Delta E = E_B - E_{\rm beam}$, where $E_{\rm beam}$ is the beam energy, and E_B and $\vec{p}_B$ are the reconstructed energy and momentum, respectively, of the B^0 candidate. All quantities are evaluated in the center-of-mass (CM) frame. To improve the $M_{\rm bc}$ resolution, the momentum $\vec{p}_B$ is calculated as $\vec{p}_B = \vec{p}_p + \vec{p}_{\bar{p}} + \frac{\vec{p}_{\pi^0}}{|\vec{p}_{\pi^0}|}\sqrt{(E_{\rm beam} - E_p - E_{\bar{p}})^2/c^2 - m^2_{\pi^0}c^2}$, where m_{π^0} is the nominal π^0 mass [2]; E_h and $\vec{p}_h$ are the energy and momentum of the hadron h ($h = p$, $\bar{p}$, π^0). In addition, a vertex fit is performed to the charged tracks to form a B^0 vertex. We require that the χ^2 from the fit be less than 200. Events with $M_{\rm bc} > 5.25$ GeV/c^2 and -0.20 GeV $< \Delta E <$ 0.15 GeV are retained for further analysis. The signal yield is calculated in a smaller region $M_{\rm bc} \in (5.272, 5.286)$ GeV/c^2 and $\Delta E \in (-0.12, +0.06)$ GeV. In order to reject contributions from charmonium states [e.g., η_c, J/ψ, $\psi(2S)$, χ_{c0}, χ_{c1}, and χ_{c2}], we apply a "charmonium veto" and exclude the regions of 2.850 GeV/c^2 $< m(p\bar{p}) <$ 3.128 GeV/c^2 and 3.315 GeV/c^2 $< m(p\bar{p}) <$ 3.735 GeV/c^2 from the event sample.

Charmless hadronic decays suffer from a large amount of continuum background, arising from light quark production ($e^+e^- \to q\bar{q}$, $q = u, d, s, c$). To suppress this background, we use a multivariate analyzer based on a neural network (NN) [17] that distinguishes jetlike continuum events from more spherical $B\bar{B}$ events. The NN uses the following input variables: the cosine of the angle between the thrust axis [18] of the B^0 candidate and the thrust axis of the rest of the event; the cosine of the angle between the B^0 thrust axis and the $+z$ axis; the cosine of the angle between the $+z$ axis and the B^0 candidate flight direction; a set of 18 modified Fox-Wolfram moments [19]; the ratio of the second to zeroth (unmodified) Fox-Wolfram moments; the separation along the z axis between the two B vertices; and the B-flavor tagging information [20]. All but for the last two quantities are evaluated in the CM frame. The NN is trained using MC simulated signal events and $q\bar{q}$ background events. The NN generates a single output variable ($C_{\rm NN}$) that ranges from -1 for backgroundlike events to $+1$ for signal-like events. We require $C_{\rm NN} > -0.5$, which rejects approximately 86% of the $q\bar{q}$ background while retaining 94% of the signal. We then translate $C_{\rm NN}$ to a new variable

$$C'_{\rm NN} = \ln\left(\frac{C_{\rm NN} - C^{\rm min}_{\rm NN}}{C^{\rm max}_{\rm NN} - C_{\rm NN}}\right), \tag{1}$$

where $C^{\rm min}_{\rm NN} = -0.5$ and $C^{\rm max}_{\rm NN} = 1.0$. This translation is advantageous as the $C'_{\rm NN}$ distribution for both signal and background is well described by a sum of Gaussian functions.

After applying all selection criteria, approximately 7% of the events have multiple B^0 candidates. For these events, we retain the candidate having the smallest sum of χ^2 values obtained from the $\pi^0 \to \gamma\gamma$ mass-constrained fit and the B^0 vertex-constrained fit. According to MC simulation, this criterion selects the correct B^0 candidate in 83% of multiple-candidate events.

We measure the signal yield by performing an unbinned extended maximum likelihood fit to the variables $M_{\rm bc}$, ΔE, and $C'_{\rm NN}$. The likelihood function is defined as

$$\mathcal{L} = e^{-\sum_j Y_j} \prod_i^N \left(\sum_j Y_j \mathcal{P}_j(M^i_{\rm bc}, \Delta E^i, C'^i_{\rm NN})\right), \tag{2}$$

where Y_j is the yield of component j; $\mathcal{P}_j(M^i_{\rm bc}, \Delta E^i, C'^i_{\rm NN})$ is the probability density function (PDF) of component j for event i, j runs over all signal and background components, and i runs over all events in the sample (N). The background components consist of continuum events, $b \to c$ (generic B) processes, and rare charmless processes. The latter two backgrounds are small compared to the continuum events and are studied using MC simulations. The rare charmless background shows a peaking structure in the $M_{\rm bc}$ distribution, most of which arises from $B^+ \to p\bar{p}\rho^+$ decays. As correlations among the variables $M_{\rm bc}$, ΔE, and $C'_{\rm NN}$ are found to be small, the three-dimensional PDFs $\mathcal{P}_j(M^i_{\rm bc}, \Delta E^i, C'^i_{\rm NN})$ are factorized into the product of separate one-dimensional PDFs.

The PDF of signal events consists of two parts: one for candidates that are correctly reconstructed, and one for those incorrectly reconstructed, i.e., at least one daughter originates from the other (tag side) B. For the former case, the $M_{\rm bc}$ and ΔE distributions are modeled with Gaussian and crystal ball [21] functions, respectively, while the $C'_{\rm NN}$ distribution is modeled with a sum of Gaussian and bifurcated Gaussian functions having a common mean. The peak positions and resolutions of the $M_{\rm bc}$, ΔE, and $C'_{\rm NN}$ PDFs are adjusted to account for data-MC differences observed in a high-statistics control

sample of $B^0 \to \bar{D}^0(\to K^+\pi^-)\pi^0$ decays. For the latter case, the correlated two-dimensional $M_{\rm bc} - \Delta E$ distribution is modeled with a nonparametric PDF [22], and the $C'_{\rm NN}$ component is modeled with a Gaussian function. The fraction of incorrectly reconstructed decays (∼4% in the signal region) is taken from MC simulation. For the rare charmless background, the $C'_{\rm NN}$ component is modeled with a bifurcated Gaussian function. The $M_{\rm bc}$ and ΔE components are modeled by a joint two-dimensional nonparametric PDF. We model the $M_{\rm bc}$, ΔE, and $C'_{\rm NN}$ distributions of continuum background with an ARGUS [23] function having its end point fixed to 5.29 GeV/c^2, a first-order polynomial, and a sum of two Gaussians having a common mean, respectively. For the generic B background, we use a bifurcated Gaussian function to model the $C'_{\rm NN}$ shape, while the similar shapes as of continuum background are used to model the $M_{\rm bc}$ and ΔE distributions. In addition to the fitted yields Y_j, all shape parameters for continuum background are also floated. All other parameters are fixed to the corresponding MC values.

The projections of the fit are shown in Fig. 1. From the fit, we extract 40.5 ± 14.2 signal events, 1490.3 ± 34.5 continuum, 100.6 ± 35.0 generic B, and 6.5 ± 10.1 rare charmless background events in the $M_{\rm bc} - \Delta E$ signal region. The resulting branching fraction is calculated as

$$\mathcal{B}(B^0 \to p\bar{p}\pi^0) = \frac{Y_{\rm sig}}{N_{B\bar{B}} \times \varepsilon}, \tag{3}$$

where $Y_{\rm sig}$ represents the extracted signal yield, $N_{B\bar{B}} = (772 \pm 11) \times 10^6$ is the total number of $B\bar{B}$ events, $\varepsilon = (10.53 \pm 0.04)\%$ is the reconstruction efficiency. The efficiency is corrected to account for possible differences in particle identification and π^0 detection efficiencies between data and simulations. In Eq. (3) we assume equal production of $B^0\bar{B}^0$ and B^+B^- pairs at the $\Upsilon(4S)$ resonance. The result is

$$\mathcal{B}(B^0 \to p\bar{p}\pi^0) = (5.0 \pm 1.8 \pm 0.6) \times 10^{-7},$$

where the first uncertainty is statistical and the second is systematic. This is the first measurement of this branching fraction.

The signal significance is calculated as $\sqrt{-2\ln(\mathcal{L}_0/\mathcal{L}_{\rm max})}$, where $\mathcal{L}_0$ is the likelihood value when the signal yield is fixed to 0, and $\mathcal{L}_{\rm max}$ is the likelihood value of the nominal fit. To include systematic uncertainties in the significance, we convolve the likelihood distribution with a Gaussian function whose width is set to the total systematic uncertainty that affects the signal yield. The resulting significance is 3.1 standard deviations. Thus, our measurement constitutes the first evidence for this decay mode.

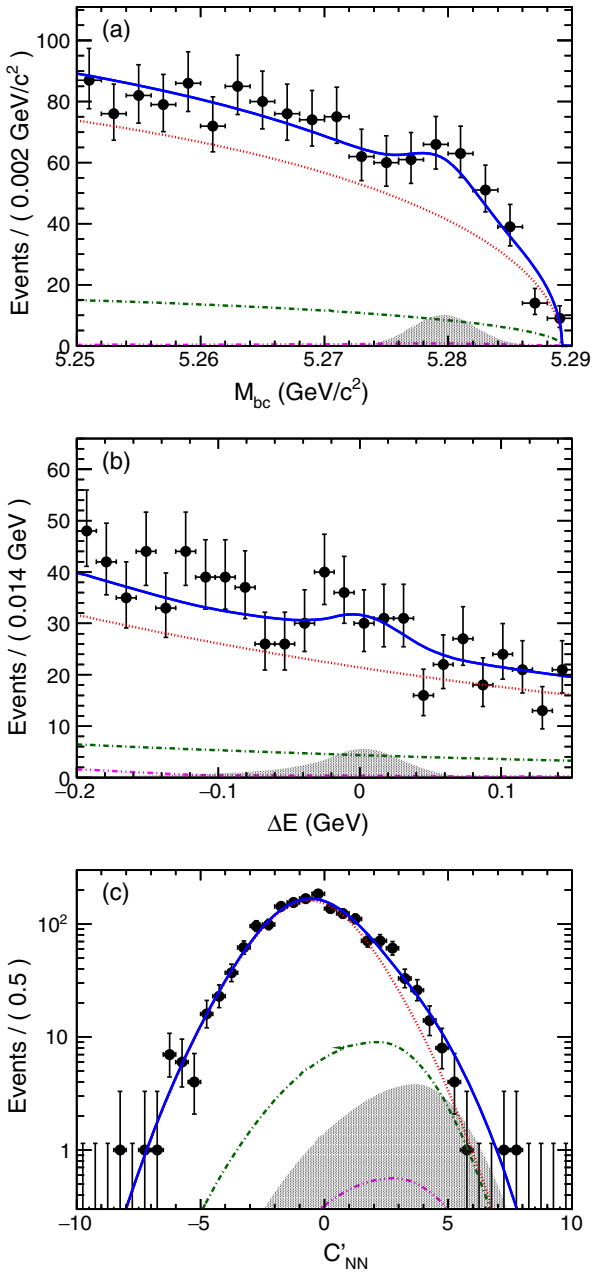

FIG. 1. Projection of the three-dimensional fit to the data: (a) $M_{\rm bc}$ in $-0.12 < \Delta E < 0.06$ GeV and $C'_{\rm NN} > 1.0$, (b) ΔE in $5.272 < M_{\rm bc} < 5.286$ GeV and $C'_{\rm NN} > 1.0$, and (c) $C'_{\rm NN}$ in $5.272 < M_{\rm bc} < 5.286$ GeV and $-0.12 < \Delta E < 0.06$ GeV. Points with error bars are data, shaded areas represent the signal, (red) dotted curves denote the continuum background, (green) dot-dashed curves the generic B background, (magenta) dot-dot-dashed curves the rare charmless background, and (blue) curves show the total contribution. The χ^2/(number of bins) values of these fit projections are 0.60, 0.83, and 0.91, respectively, which indicates that the fit gives a good description of the data.

The systematic uncertainty in $\mathcal{B}(B^0 \to p\bar{p}\pi^0)$ arises from several sources, as listed in Table I. The uncertainty due to the fixed parameters in the PDF is estimated by varying them individually according to their statistical uncertainties.

TABLE I. Systematic uncertainties in $\mathcal{B}(B^0 \to p\bar{p}\pi^0)$. Those listed in the upper section are associated with fitting for the signal yields and are included in the signal significance.

Source	Uncertainty (%)
PDF parametrization	$^{+2.9}_{-3.2}$
Calibration factor	11.9
Fit bias	$^{+2.1}_{-0.0}$
π^0 reconstruction	1.5
Tracking	0.7
Particle identification	0.6
Choice of $C_{\rm NN}$	$^{+2.0}_{-1.1}$
Incorrectly reconstructed signal events	$^{+1.0}_{-0.8}$
Number of $B\bar{B}$ pairs	1.4
MC statistics	0.4
Total	$^{+12.8}_{-12.6}$

For each variation, the branching fraction is recalculated, and the difference with the nominal value is taken as the systematic uncertainty associated with that parameter. The smoothing parameters of the nonparametric functions are also varied. The differences in the fit results are included as systematic uncertainties. We add all uncertainties in quadrature to obtain the overall uncertainty due to PDF parametrization. The uncertainties due to errors in the calibration factors used to account for data-MC differences in the signal PDF are evaluated separately but in a similar manner. To test the stability of our fitting procedure, we generate and fit a large ensemble of pseudoexperiments. We find a potential fit bias of $+2.1\%$. We attribute this bias to neglecting small correlations among the fitted observables. We assign a 1.5% systematic uncertainty due to π^0 reconstruction; this is determined from a study of $\tau^- \to \pi^-\pi^0\nu_\tau$ decays [24]. The systematic uncertainty due to the track reconstruction efficiency is 0.35% per track, as determined from a study of partially reconstructed $D^{*+} \to D^0\pi^+$, $D^0 \to K^0_S\pi^+\pi^-$ decays. A 0.6% systematic uncertainty is assigned due to the particle identification efficiency of the proton-antiproton pair; this is determined from a study of $\Lambda \to p\pi^-$ decays. We determine the systematic uncertainty due to the $C_{\rm NN}$ selection by applying different $C_{\rm NN}$ criteria and comparing the results with that of the $C_{\rm NN}$ nominal selection. The uncertainty due to the estimated fraction of incorrectly reconstructed signal events is obtained by varying this fraction by $\pm 50\%$. The systematic uncertainty due to the counting of the total number of $B\bar{B}$ pairs is 1.4%, and the uncertainty due to the finite statistics of the simulated signal sample used to evaluate the reconstructed efficiency is 0.4%. The total systematic uncertainty is obtained by adding each source in quadrature, as they are assumed to be uncorrelated.

Figure 2 shows the background-subtracted and efficiency-corrected distribution of $m(p\bar{p})$, where the charmonium veto is removed. For the background subtraction, we use the *sPlot* technique [25], with $M_{\rm bc}$, ΔE, and $C'_{\rm NN}$ as the discriminating variables. As expected, an enhancement near threshold is visible. The background-subtracted distributions of $m(p\pi^0)$ and $m(\bar{p}\pi^0)$ are shown in Fig. 3. No obvious structure is seen in these distributions.

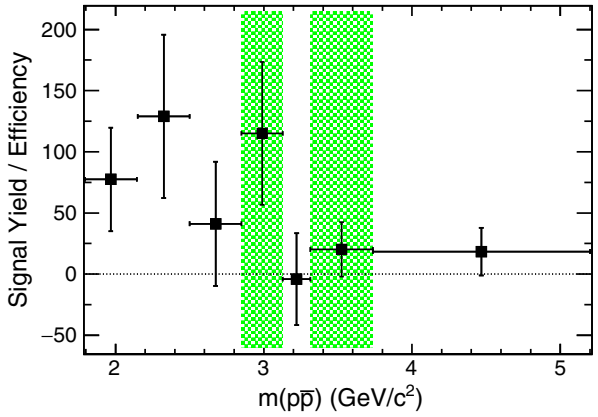

FIG. 2. Background-subtracted and efficiency-corrected distribution of $m(p\bar{p})$. Points with error bars are the data and (green) shaded regions represent the area of charmonium veto.

We also search for the intermediate two-body decay $B^0 \to \Delta^+(\to p\pi^0)\bar{p}$. Events with $m(p\pi^0) < 1.4$ GeV/c^2 are selected for this search. No significant signal is observed in this mass range. We set an upper limit on the branching fraction of $B^0 \to \Delta^+\bar{p}$ at 90% confidence level (C.L.) using a Bayesian approach. The limit is obtained by integrating the likelihood function from 0 to infinity; the value that corresponds to 90% of this total area is taken as the 90% C.L. upper limit. We include the systematic uncertainty in the calculation by convolving the likelihood distribution with a Gaussian function whose width is set equal to the total systematic uncertainty of $\mathcal{B}(B^0 \to p\bar{p}\pi^0)$. As we do not know the flavor of the B

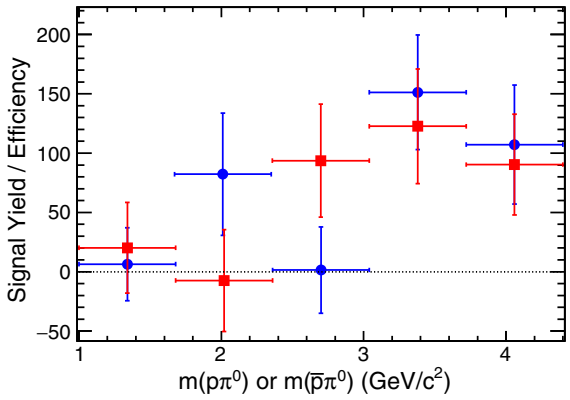

FIG. 3. Background-subtracted and efficiency-corrected distributions of $m(p\pi^0)$ and $m(\bar{p}\pi^0)$. The (blue) circles represent $m(p\pi^0)$ and (red) squares the $m(\bar{p}\pi^0)$. The charmonium veto is not applied in this plot.

meson at decay, we express our result as a sum of final states containing either a Δ^+ or a $\bar{\Delta}^-$. The result is

$$\mathcal{B}(B^0 \to \Delta^+ \bar{p}) + \mathcal{B}(B^0 \to \bar{\Delta}^- p) < 1.6 \times 10^{-6}.$$

This is the first such limit and is in agreement with the theoretical predictions [3,26].

In summary, using the full set of Belle data, we report a measurement of the branching fraction for $B^0 \to p\bar{p}\pi^0$ decays. We obtain $\mathcal{B}(B^0 \to p\bar{p}\pi^0) = (5.0 \pm 1.8 \pm 0.6) \times 10^{-7}$, where the first uncertainty is statistical and the second is systematic. The significance of this result is 3.1 standard deviations, and thus this measurement constitutes the first evidence for this decay. We also search for the intermediate two-body decays $B^0 \to \Delta^+ \bar{p}$ and $B^0 \to \bar{\Delta}^- p$, and set an upper limit on the branching fraction, $\mathcal{B}(B^0 \to \Delta^+ \bar{p}) + \mathcal{B}(B^0 \to \bar{\Delta}^- p) < 1.6 \times 10^{-6}$ at 90% C.L.

ACKNOWLEDGMENTS

We thank the KEKB group for the excellent operation of the accelerator; the KEK cryogenics group for the efficient operation of the solenoid; and the KEK computer group, and the Pacific Northwest National Laboratory (PNNL) Environmental Molecular Sciences Laboratory (EMSL) computing group for strong computing support; and the National Institute of Informatics, and Science Information NETwork 5 (SINET5) for valuable network support. We acknowledge support from the Ministry of Education, Culture, Sports, Science, and Technology (MEXT) of Japan, the Japan Society for the Promotion of Science (JSPS), and the Tau-Lepton Physics Research Center of Nagoya University; the Australian Research Council including Grants No. DP180102629, No. DP170102389, No. DP170102204, No. DP150103061, No. FT130100303; Austrian Science Fund under Grant No. P 26794-N20; the National Natural Science Foundation of China under Contracts No. 11435013, No. 11475187, No. 11521505, No. 11575017, No. 11675166, No. 11705209; Key Research Program of Frontier Sciences, Chinese Academy of Sciences (CAS), Grant No. QYZDJ-SSW-SLH011; the CAS Center for Excellence in Particle Physics (CCEPP); the Shanghai Pujiang Program under Grant No. 18PJ1401000; the Ministry of Education, Youth and Sports of the Czech Republic under Contract No. LTT17020; the Carl Zeiss Foundation, the Deutsche Forschungsgemeinschaft, the Excellence Cluster Universe, and the VolkswagenStiftung; the Department of Science and Technology of India; the Istituto Nazionale di Fisica Nucleare of Italy; National Research Foundation (NRF) of Korea Grants No. 2015H1A2A1033649, No. 2016R1D1A1B01010135, No. 2016K1A3A7A09005 603, No. 2016R1D1A1B02012900, No. 2018R1A2B3003 643, No. 2018R1A6A1A06024970, No. 2018R1D1 A1B07047294; Radiation Science Research Institute, Foreign Large-size Research Facility Application Supporting project, the Global Science Experimental Data Hub Center of the Korea Institute of Science and Technology Information and KREONET/GLORIAD; the Polish Ministry of Science and Higher Education and the National Science Center; the Grant of the Russian Federation Government, Grant No. 14.W03.31.0026; the Slovenian Research Agency; Ikerbasque, Basque Foundation for Science, Spain; the Swiss National Science Foundation; the Ministry of Education and the Ministry of Science and Technology of Taiwan; and the United States Department of Energy and the National Science Foundation.

[1] K. Abe *et al.* (Belle Collaboration), Observation of $B^\pm \to p\bar{p}K^\pm$, Phys. Rev. Lett. **88**, 181803 (2002).
[2] M. Tanabashi *et al.* (Particle Data Group), Review of particle physics, Phys. Rev. D **98**, 030001 (2018).
[3] H. Y. Cheng and K. C. Yang, Charmless exclusive baryonic B decays, Phys. Rev. D **66**, 014020 (2002).
[4] H. Y. Cheng and C. K. Chua, On the smallness of tree-dominated charmless two-body baryonic B decay rates, Phys. Rev. D **91**, 036003 (2015).
[5] W. S. Hou and A. Soni, Pathways to Rare Baryonic B Decays, Phys. Rev. Lett. **86**, 4247 (2001).
[6] C. H. Chen, H. Y. Cheng, C. Q. Geng, and Y. K. Hsiao, Charmful three-body baryonic B decays, Phys. Rev. D **78**, 054016 (2008).
[7] J. Haidenbauer, U. G. Meissner, and A. Sibirtsev, Near threshold $p\bar{p}$ enhancement in B and J/ψ decay, Phys. Rev. D **74**, 017501 (2006).
[8] H. Y. Cheng, Exclusive baryonic B decays Circa 2005, Int. J. Mod. Phys. A **21**, 4209 (2006).
[9] V. Laporta, Final stare interaction enhancement effect on the near threshold $p\bar{p}$ system in $B^+ \to p\bar{p}\pi^+$ decay, Int. J. Mod. Phys. A **22**, 5401 (2007).
[10] R. Aaij *et al.* (LHCb Collaboration), Evidence for CP Violation in $B^+ \to p\bar{p}K^+$ Decays, Phys. Rev. Lett. **113**, 141801 (2014).
[11] Unless stated otherwise, charge-conjugate modes are implicitly included.
[12] A. Abashian *et al.* (Belle Collaboration), The Belle detector, Nucl. Instrum. Methods Phys. Res., Sect. A **479**, 117 (2002); also see the detector section in J. Brodzicka *et al.* (Belle Collaboration), Physics achievements from the Belle experiment, Prog. Theor. Exp. Phys. **2012**, 4D001 (2012).
[13] S. Kurokawa and E. Kikutani, Overview of the KEKB accelerators, Nucl. Instrum. Methods Phys. Res., Sect. A

499, 1 (2003), and other papers included in this Volume; T. Abe *et al.*, Achievements of KEKB, Prog. Theor. Exp. Phys. **2013**, 03A011 (2013) and references therein.

[14] D. J. Lange, The EvtGen particle decay simulation package, Nucl. Instrum. Methods Phys. Res., Sect. A **462**, 152 (2001).

[15] R. Brun *et al.*, GEANT 3.21, CERN Report No. DD/EE/84-1, 1984.

[16] P. Golonka and Z. Was, Photos Monte Carlo: A precision tool for QED corrections in Z and W decays, Eur. Phys. J. C **45**, 97 (2006).

[17] M. Feindt and U. Kerzel, The NeuroBayes neural network package, Nucl. Instrum. Methods Phys. Res., Sect. A **559**, 190 (2006).

[18] S. Brandt, C. Peyrou, R. Sosnowski, and A. Wroblewski, The principal axis of jets. An attempt to analyze high-energy collisions as two-body processes, Phys. Lett. **12**, 57 (1964).

[19] G. C. Fox and S. Wolfram, Observables for the Analysis of Event Shapes in e^+e^- Annihilation and Other Processes, Phys. Rev. Lett. **41**, 1581 (1978); The modified moments used in this Letter are described in S. H. Lee *et al.* (Belle Collaboration), Evidence for $B^0 \to \pi^0\pi^0$, Phys. Rev. Lett. **91**, 261801 (2003).

[20] H. Kakuno *et al.* (Belle Collaboration), Neutral B flavor tagging for the measurement of mixing induced CP violation at Belle, Nucl. Instrum. Methods Phys. Res., Sect. A **533**, 516 (2004).

[21] T. Skwarnicki, A study of the radiative Cascade transitions between the Upsilon-prime and Upsilon resonances, CERN Report No. DESY-F31-86-02, 1986.

[22] K. S. Cranmer, Kernel estimation in high energy physics, Comput. Phys. Commun. **136**, 198 (2001).

[23] H. Albrecht *et al.* (ARGUS Collaboration), Search for hadronic $b \to u$ decays, Phys. Lett. B **241**, 278 (1990).

[24] S. Ryu *et al.* (Belle Collaboration), Measurements of branching fractions of τ lepton decays with one or more K^0_S, Phys. Rev. D **89**, 072009 (2014).

[25] M. Pivk and F. R. Le Diberder, sPlot: A statistical tool to unfold data distributions, Nucl. Instrum. Methods Phys. Res., Sect. A **555**, 356 (2005).

[26] V. L. Chernyak and I. R. Zhitnitsky, B meson exclusive decays into baryons, Nucl. Phys. **B345**, 137 (1990).